

Influence of Roughness and Disorder on Tunneling Magnetoresistance

P. X. Xu,¹ V. M. Karpan,² K. Xia,¹ M. Zwierzycki,^{2,3} I. Marushchenko,² and P. J. Kelly²

¹*Beijing National Laboratory for Condensed Matter Physics,*

Institute of Physics, Chinese Academy of Sciences, Beijing 100080, China

²*Faculty of Science and Technology and MESA⁺ Institute for Nanotechnology,*

University of Twente, P.O. Box 217, 7500 AE Enschede, The Netherlands

³*Max-Planck-Institut für Festkörperforschung, Heisenbergstr. 1, D-70569 Stuttgart, Germany.*

(Dated: April 10, 2018)

A systematic, quantitative study of the effect of interface roughness and disorder on the magnetoresistance of FeCo|vacuum|FeCo magnetic tunnel junctions is presented based upon parameter-free electronic structure calculations. Surface roughness is found to have a very strong effect on the spin-polarized transport while that of disorder in the leads (leads consisting of a substitutional alloy) is weaker but still sufficient to suppress the huge tunneling magneto-resistance (TMR) predicted for ideal systems.

Tunneling magnetoresistance (TMR) refers to the dependence of the resistance of a FM₁|I|FM₂ (ferromagnet|insulator|ferromagnet) magnetic tunnel junction (MTJ) on the relative orientation of the magnetization directions of the ferromagnetic electrodes when these are changed from being antiparallel (AP) to parallel (P): $TMR = (R_{AP} - R_P)/R_P \equiv (G_P - G_{AP})/G_{AP}$. Since the discovery of large values of TMR in MTJs based upon ultrathin layers of amorphous Al₂O₃ as insulator,¹ a considerable effort has been devoted to exploiting the effect in sensors and as the basis for non-volatile memory elements. Understanding TMR has been complicated by the difficulty of experimentally characterizing FM|I interfaces. The chemical composition of the interface has been shown² to have a strong influence on the magnitude and polarization of the TMR and knowledge of the interface structure is a necessary preliminary to analyzing MTJs theoretically. In the absence of detailed structural models of the junctions and the materials-specific electronic structures which could be calculated with such models, the effect was interpreted in terms of electrode conduction-electron spin polarizations P_i , using a model suggested by Julliere³ in which the $TMR = 2P_1P_2/(1 - P_1P_2)$. A great deal of discussion has focussed on the factors contributing to the quantity⁴ P but the use of amorphous oxide as barrier material made impossible a detailed theoretical study with which to confront experiment.^{6,7}

The situation changed quite drastically with the recent observation of large values of TMR at room temperature in FeCo|MgO|FeCo MTJs in which the MgO tunnel barrier was mono-^{8,9} or poly-crystalline.¹⁰ This work was motivated in part by the prediction^{11,12} by materials-specific transport calculations of huge TMR values for ideal Fe|MgO|Fe structures. This new development lends fresh urgency to the need to understand the factors governing the sign and magnitude of TMR because the largest observed value of 353% at low temperature,⁹ is still well below the ab-initio predicted values of order 10,000% for the relevant thicknesses of MgO.¹¹ Some effort has been devoted to explaining the discrepancy in terms of interface relaxation¹³ or the formation of a layer

of FeO at the interface^{14,15} but the role of interface disorder has only been speculated upon.¹⁶

Method. In this paper, we use first principles electronic structure calculations to study the effect of roughness and alloy disorder on TMR in MTJs with a vacuum barrier and Fe_{1-x}Co_x alloy electrodes. A vacuum barrier was chosen for its simplicity and because there are many studies of spin-dependent vacuum tunneling in its own right.^{17,18,19,20,21} We consider the effect of diffusive scattering in the linear-response regime in a two-step procedure. In the first step, the electronic structure of the Fe_{1-x}Co_x|vacuum|Fe_{1-x}Co_x MTJ is determined using the local-density approximation²² of density functional theory. The self-consistent calculations are performed with the tight-binding linear muffin-tin orbital (TB-LMTO)²³ surface Green's function method²⁴ and disordered systems are treated using the layer CPA (coherent potential approximation).²⁵ The atomic sphere (AS) potentials serve as input to the second step in which the transmission matrix entering Landauer's transport formalism²⁶ is calculated using a TB-MTO implementation^{27,28} of a wave-function matching scheme due to Ando.²⁹ Disorder is modelled in large lateral supercells by distributing the self-consistently calculated CPA-AS potentials at random, layer-for-layer in the appropriate concentrations for as many configurations as are required. In most of the calculations to be presented, supercells containing 10 × 10 atoms per monatomic layer were used.

We consider transport in the (001) growth direction keeping atoms at the surfaces unrelaxed in their bulk bcc positions. For Fe leads the experimental lattice constant $a_{Fe} = 2.866\text{\AA}$ is used. For Co leads $a_{Co} = 2.817\text{\AA}$ is chosen so that the bcc lattice has the same volume as hcp Co. The alloy is considered to obey Vegard's law whereby

$$a_{Fe_{1-x}Co_x} = (1 - x)a_{Fe} + xa_{Co} \quad (1)$$

The vacuum region is modelled in the atomic spheres approximation (ASA) by filling the space between the leads with 'empty' spheres of the same size³⁰ and on the same

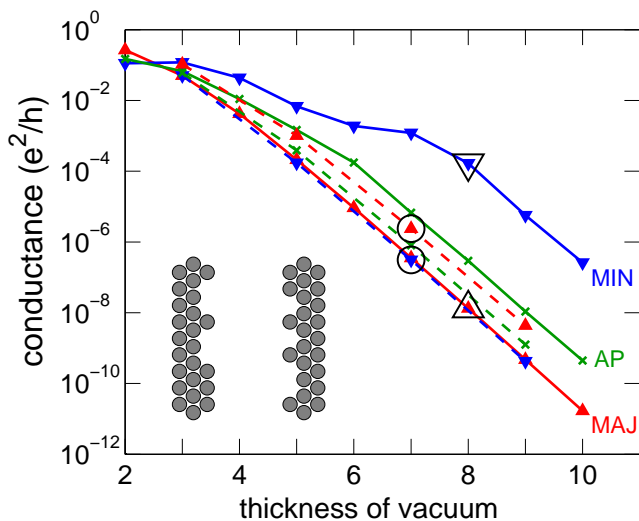


FIG. 1: (Color online) Conductances G_P^{min} (\blacktriangledown), G_P^{maj} (\blacktriangle), and G_{AP}^σ (\times) of an Fe|vacuum|Fe MTJ as a function of the barrier thickness (measured in units of layers of a bcc lattice). The solid lines are for ideal junctions. The dashed lines are configuration-averaged conductances for rough junctions prepared by removing, at random, half of the Fe atoms from one surface and depositing them, at random, on the other surface. The results are normalized to the 1×1 surface unit cell used for the ideal case. The large symbols refer to data points which also appear in the next figure.

bcc lattice as in the leads. Consequently we measure the thickness of the vacuum barrier in monolayers (MLs) of empty atomic spheres.

Ideal Fe|vac|Fe. The conductances G_P^σ and G_{AP}^σ for an ideal, ordered Fe|vacuum|Fe MTJ are shown in Fig. 1 (solid lines) as a function of the width of the barrier for the minority and majority spin channels, $\sigma = min, maj$. In all three cases an exponential dependence on the barrier width is reached asymptotically. For G_P^{maj} , the asymptotic dependence sets in after about five MLs of vacuum; the initial subexponential behaviour is related to the deviation of the barrier from a simple step form. The behaviour of G_P^{min} is much more complex, becoming exponential only when the vacuum is some 8 MLs or more thick; the AP case is intermediate. The TMR increases³¹ as a function of the width of the vacuum barrier reaching huge asymptotic values of order 20,000%, similar in size to those reported^{11,12} for Fe|MgO|Fe. The non-trivial dependence of G_P^{min} on barrier width can be understood in terms of a surface state¹⁷ at $\bar{\Gamma}$ ($\mathbf{k}_\parallel = 0$) which is very close to the Fermi level in the minority spin channel of iron but well below it for majority spin electrons. In the P configuration one such state exists on each surface and at values of $\mathbf{k}_\parallel \neq 0$ these states become surface resonances which form bonding-antibonding pairs with transmission probabilities close to unity.³³ As the vacuum barrier is widened, the coupling between the surface resonances weakens until the bonding-antibonding splitting becomes smaller than the resonance width at which

point the maximum transmission becomes smaller than unity and normal exponential dependence of the conductance on the barrier width sets in; the asymptotic slope in Fig. 1 is consistent with our calculated Fe workfunction of 4.7 eV.

Roughness: 50% coverage. An ideal tunnel junction such as that just considered is impossible to realize in practice; there will always be some finite amount of disorder whether it be surface roughness, islands, dislocations etc. A more realistic model is obtained by considering an Fe|vacuum|Fe system with incomplete (rough) surface layers, modelled by occupying, at random, a fraction of the lattice sites of the topmost layer with Fe atoms (see the inset in Fig. 1) and using the layer CPA to determine the corresponding AS potentials.

Roughness resulting from depositing some Fe atoms on an ideal surface has two effects. The first is to destroy the point group symmetry which led to the existence of a symmetry gap at $\bar{\Gamma}$ for states with Δ_1 symmetry, and thus the surface state with that symmetry. We expect this to reduce the large minority spin conductance found for the ideal vacuum barrier. The second effect of roughness is to reduce the width of the vacuum barrier and thus to enhance the conductance which depends exponentially on the barrier width.

These competing effects are disentangled by starting with an ideal vacuum barrier and moving half of the Fe atoms from one surface and depositing them on the other so that the barrier width is, on average, unchanged. The results of these supercell calculations, averaged over 20 configurations and normalized to the ideal MTJ (1×1 surface unit cell) results are included in Fig. 1. The contribution of the interface states to G_P^{min} is completely quenched by the roughness and the conductance reduced by four orders of magnitude. G_P^{maj} is enhanced by about an order of magnitude because the increased conductance from those parts of the rough surfaces which are closer than average more than compensates the decreased conductance from part of the rough surfaces which are further away than average. All conductances now exhibit the same qualitative behavior: exponential decay. Not only is the absolute value of the TMR greatly reduced by roughness, the sign of the polarization is reversed.

This result immediately prompts us to ask how the TMR depends on the amount of roughness and, in particular, what coverage is needed to suppress the contribution of the resonances to G_P^{min} . This issue is addressed in Fig. 2 where the conductance of a MTJ is shown as a function of surface coverage. Zero coverage corresponds to an ideal MTJ with 8 MLs vacuum; 100% coverage (not shown) to 6 MLs. We see that 5% coverage is sufficient to reduce G_P^{min} , and the TMR, by two orders of magnitude. Unless the surface roughness is less than a few percent, the TMR lies between about 10 and 1000% (Fig. 2, inset), comparable to values observed in experiment. As G_P^{min} is reduced by roughness, G_P^{maj} increases monotonically with increasing coverage as the average barrier width decreases; the two cross at a surface coverage of about 25%.

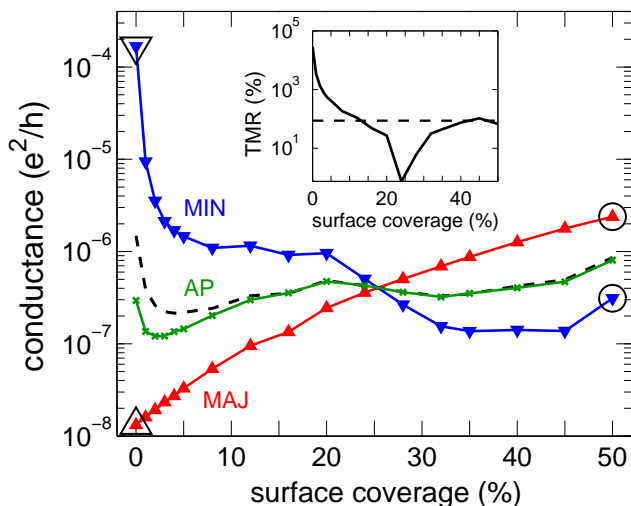


FIG. 2: (Color online) Configuration-averaged conductances G_P^{min} (\blacktriangledown), G_P^{maj} (\blacktriangle), and G_{AP}^σ (\times) of an Fe|vacuum|Fe MTJ with 8 ML thick vacuum barrier as a function of the surface coverage, normalized to a 1×1 surface unit cell. The dashed line denotes G_{AP}^σ predicted from Eq. 2. Large symbols refer to the similarly marked data points in the previous figure. Inset: TMR as a function of the surface coverage. The dashed line is the value predicted using Julliere's expression and a calculated DOS polarization of 55%.

The single spin AP conductance, G_{AP}^σ , is described qualitatively very well for all coverages by the relation³⁴

$$G_{AP}^\sigma = \sqrt{G_P^{maj} G_P^{min}} \quad (2)$$

(dashed line in Fig. 2) and quantitatively for coverages greater than a few percent i.e., as soon as the surface resonance contribution is killed by roughness.³⁵ When Eq. (2) holds, $G_P \equiv G_P^{maj} + G_P^{min}$ is greater than $G_{AP}^\sigma \equiv 2G_{AP}^\sigma$ and the TMR is always positive although the polarization in the P configuration changes sign, reaching its minimum value at 25% coverage where G_P^{maj} and G_P^{min} crossover.

As long as there is enough roughness to quench the surface resonance, there is order-of-magnitude agreement between our TMR calculated as a function of surface roughness and the value obtained using Julliere's expression for the TMR with the calculated, bulk density-of-states polarization for Fe, $P = 55\%$, shown as a dashed line in the inset to Fig. 2.

Disorder in the leads. It is interesting to study an intermediate type of disorder where there is no roughness but the electrodes are made of a substitutional $\text{Fe}_{1-x}\text{Co}_x$ magnetic alloy. As the alloy concentration x is increased, the disorder increases but the underlying electronic structure is also changing as the Fermi energy rises. To distinguish these two effects, we first carry out calculations for a VCA|vac|VCA MTJ in which the $\text{Fe}_{1-x}\text{Co}_x$ electrodes are treated within the virtual

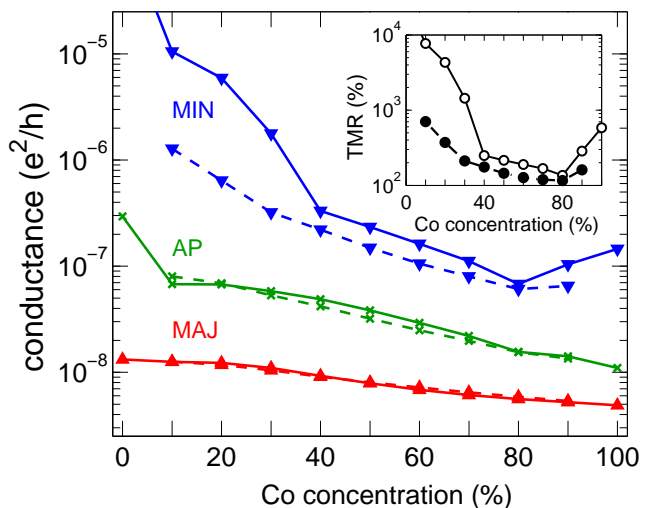


FIG. 3: (Color online) G_P^{min} (\blacktriangledown), G_P^{maj} (\blacktriangle), and G_{AP}^σ (\times) for an $\text{Fe}_{1-x}\text{Co}_x$ |vacuum| $\text{Fe}_{1-x}\text{Co}_x$ MTJ with 8 ML thick vacuum barrier as a function of x , the concentration of Co atoms, calculated in the virtual crystal (VCA: solid lines) and CPA/supercell (SC: dashed lines) approximations. Conductances are configuration averaged and normalized to a 1×1 surface unit cell. Inset: TMR in VCA (\circ) and CPA/SC (\bullet) approximations.

crystal approximation (VCA). This allows us to probe the effect of changing the Fermi energy without including disorder. It turns out to be also very convenient to embed $\text{Fe}_{1-x}\text{Co}_x$ |vac| $\text{Fe}_{1-x}\text{Co}_x$ between VCA leads (schematically denoted) as VCA|CPA|vac|CPA|VCA for performing the self-consistent potential calculations and as VCA|SC|vac|SC|VCA for the conductance calculation where, as before, CPA potentials are used as input to the supercell (SC) transport calculations. Details of the thicknesses of the various regions needed to achieve converged results as well as the number of k-points, supercell sizes and other technical details will be given in a forthcoming publication.

The results of these calculations are shown in Fig. 3. G_P^{maj} and G_{AP}^σ are unchanged by disorder within the accuracy of the calculation. The largest change can once again be seen in G_P^{min} . In the case of ideal VCA electrodes, there are localized surface states in the minority channel as one would expect. With increasing Co concentration x , the Fermi level rises with respect to these surface states, resulting in a decreasing contribution to the conductance from the surface resonances. This is clearly demonstrated by the behavior of G_P^{min} in Fig. 3. Lead disorder quenches the contribution of the resonant states by destroying the point group symmetry, eliminating the symmetry gap and broadening the resonances. At a concentration of about 40%, the surface resonances are no longer dominant and the effect of disorder is quite small; for $x \geq 0.4$ the trend as a function of x is described quite well by the VCA calculation. Eq. (2) is again found to describe the AP conductance very well. We see thus that

lead disorder has the same effect as roughness in quenching the huge values of TMR (inset to Fig. 3) found for the disorder-free VCA reference system, albeit less effectively.

Summary. Using first-principles calculations we find that both roughness and alloy disorder quench the TMR for ideal magnetic tunnel junctions to values comparable to the highest found experimentally for monocrySTALLINE barrier materials or vacuum tunneling. We therefore propose that these experiments are still in the roughness/disorder limited regime.

This work is part of the research program of the “Stichting voor Fundamenteel Onderzoek der Materie”

(FOM) and the use of supercomputer facilities was sponsored by the “Stichting Nationale Computer Faciliteiten” (NCF), both financially supported by the “Nederlandse Organisatie voor Wetenschappelijk Onderzoek” (NWO). VMK is supported by “NanoNed”, a Nanotechnology programme of the Dutch Ministry of Economic Affairs. KX acknowledges support from NSF of China, Grant No. 90303014.

We are grateful to Anton Starikov for permission to use his version of the TB-MTO code based upon sparse matrix techniques with which we performed some of the calculations.

-
- ¹ J. S. Moodera, L. R. Kinder, T. M. Wong, and R. Meserve, *Phys. Rev. Lett.* **74**, 3273 (1995).
- ² J. M. De Teresa, A. Barthélémy, A. Fert, J. P. Contour, F. Montaigne, and P. Seneor, *Science* **286**, 507 (1999).
- ³ M. Julliere, *Phys. Lett. A* **54**, 225 (1975).
- ⁴ P_i was not defined strictly in Ref. 3 and it has frequently been interpreted in terms of the density-of-states polarization $P = [D_{\uparrow}(\varepsilon_f) - D_{\downarrow}(\varepsilon_f)]/[D_{\uparrow}(\varepsilon_f) + D_{\downarrow}(\varepsilon_f)]$ where $D_{\sigma}(\varepsilon)$ is a bulk density of states. It has been pointed out⁵ that other measures of the spin polarization may be more appropriate when studying transport.
- ⁵ I. I. Mazin, *Phys. Rev. Lett.* **83**, 1427 (1999).
- ⁶ E. Y. Tsymbal, O. N. Mryasov, and P. R. LeClair, *J. Phys.: Condens. Matter.* **15**, R109 (2003).
- ⁷ X. G. Zhang and W. H. Butler, *J. Phys.: Condens. Matter.* **15**, R1603 (2003).
- ⁸ S. Yuasa, T. Nagahama, A. Fukushima, Y. Suzuki, and K. Ando, *Nature Materials* **3**, 868 (2004).
- ⁹ S. Yuasa, T. Katayama, T. Nagahama, A. Fukushima, H. Kubota, Y. Suzuki, and K. Ando, *Appl. Phys. Lett.* **87**, 222508 (2005).
- ¹⁰ S. S. P. Parkin, C. Kaiser, A. Panchula, P. M. Rice, B. Hughes, M. Samant, and S. H. Yang, *Nature Materials* **3**, 862 (2004).
- ¹¹ W. H. Butler, X.-G. Zhang, T. C. Schulthess, and J. M. MacLaren, *Phys. Rev. B* **63**, 054416 (2001).
- ¹² J. Mathon and A. Umerski, *Phys. Rev. B* **63**, 220403 (2001).
- ¹³ D. Wortmann, G. Bihlmayer, and S. Blügel, *J. Phys.: Condens. Matter.* **16**, s5819 (2004).
- ¹⁴ X. G. Zhang, W. H. Butler, and A. Bandyopadhyay, *Phys. Rev. B* **68**, 092402 (2003).
- ¹⁵ C. Tusche, H. L. Meyerheim, N. Jedrecy, G. Renaud, A. Ernst, J. Henk, P. Bruno, and J. Kirschner, *Phys. Rev. Lett.* **95**, 176101 (2005).
- ¹⁶ K. D. Belashchenko, J. Velez, and E. Y. Tsymbal, *Phys. Rev. B* **72**, 140404 (2005).
- ¹⁷ J. A. Stroschio, D. T. Pierce, A. Davies, R. J. Celotta, and M. Weinert, *Phys. Rev. Lett.* **75**, 2960 (1995).
- ¹⁸ S. F. Alvarado, *Phys. Rev. Lett.* **75**, 513 (1995).
- ¹⁹ S. N. Okuno, T. Kishi, and K. Tanaka, *Phys. Rev. Lett.* **88**, 066803 (2002).
- ²⁰ H. F. Ding, W. Wulfhekel, J. Henk, P. Bruno, and J. Kirschner, *Phys. Rev. Lett.* **90**, 116603 (2003).
- ²¹ M. M. J. Bischoff, T. K. Yamada, C. M. Fang, R. A. de Groot, and H. van Kempen, *Phys. Rev. B* **68**, 045422 (2003).
- ²² U. von Barth and L. Hedin, *J. Phys. C: Sol. State Phys.* **5**, 1629 (1972).
- ²³ O. K. Andersen, Z. Pawłowska, and O. Jepsen, *Phys. Rev. B* **34**, 5253 (1986).
- ²⁴ I. Turek, V. Drchal, J. Kudrnovský, M. Šob, and P. Weinberger, *Electronic Structure of Disordered Alloys, Surfaces and Interfaces* (Kluwer, Boston-London-Dordrecht, 1997).
- ²⁵ P. Soven, *Phys. Rev.* **156**, 809 (1967).
- ²⁶ S. Datta, *Electronic Transport in Mesoscopic Systems* (Cambridge University Press, Cambridge, 1995).
- ²⁷ K. Xia, P. J. Kelly, G. E. W. Bauer, I. Turek, J. Kudrnovský, and V. Drchal, *Phys. Rev. B* **63**, 064407 (2001).
- ²⁸ K. Xia, M. Zwierzycki, M. Talanana, P. J. Kelly, and G. E. W. Bauer, *Phys. Rev. B* **73**, 064420 (2006).
- ²⁹ T. Ando, *Phys. Rev. B* **44**, 8017 (1991).
- ³⁰ The Fe and Co lattice constants correspond to Wigner-Seitz atomic sphere radii of 2.667 and 2.621 Bohr atomic units, respectively.
- ³¹ The conductance polarization changes sign from positive to negative as the vacuum separation is increased. The positive polarization found by MacLaren *et al.*³² can be reproduced by using non selfconsistent potentials and small number of k points.
- ³² J. M. MacLaren, X.-G. Zhang, and W. H. Butler, *Phys. Rev. B* **56**, 11827 (1997).
- ³³ O. Wunnicke, N. Papanikolaou, R. Zeller, P. H. Dederichs, V. Drchal, and J. Kudrnovský, *Phys. Rev. B* **65**, 064425 (2002).
- ³⁴ K. D. Belashchenko, E. Y. Tsymbal, M. van Schilfhaarde, D. A. Stewart, I. I. Oleynik, and S. S. Jaswal, *Phys. Rev. B* **69**, 174408 (2004).
- ³⁵ For ideal MTJs, the resonant tunneling contribution will be quenched for sufficiently thick barriers so Eq. (2) can also be expected to hold in that situation.